Supporting Information

Molecular Design and Synthesis of a pH Independent and Cell Permeant Fluorescent Dye and its Applications

Xiaojie Jiao,[†] Chang Liu,[†, ‡] Kun Huang,[†, ‡] Siwen Zhang,[†] Song He,[†] Liancheng Zhao[†, ‡] and Xianshun Zeng*[†]

[†] Tianjin Key Laboratory for Photoelectric Materials and Devices, School of Material Science and Engineering, Tianjin University of Technology, Tianjin 300384, China.

[‡] School of Materials Science and Engineering, Institute of Information Functional Materials & Devices, Harbin Institute of Technology, Harbin 150001, China.

Table S1 Absorbance and emission properties of the dye **1** in different solvents.

solvents	$\lambda_{abs}(\varepsilon)$		λ_{em}	solvents	$\lambda_{abs}(\varepsilon)$		λ_{em}
	-TFA[a]	+TFA[b]			-TFA	+TFA	
C_7H_8	582(200)	582(45800)	624	CH_3CN	576(400)	576(52400)	618
CH_2Cl_2	581(2400)	581（66000）	619	CH_3OH	568(12000)	579(63000)	622
THF	--[c]	582(29700)	621	EtOH	575(1100)	581(68500)	625
AcOEt	579(100)	579(42800)	619	DMSO	592(1500)	587(39700)	632
$CHCl_3$	--	581(64000)	624	DMF	--	584(46300)	629
$C_4H_8O_2$	568(1000)	578(7600)	621	H_2O	572(38100)	576(38400)	620
C_3H_6O	578(300)	578(47800)	620				

Notes: a: “-TFA”without TFA; b: “+TFA”with 1% TFA; c: “--” means the absorbance value is negative.

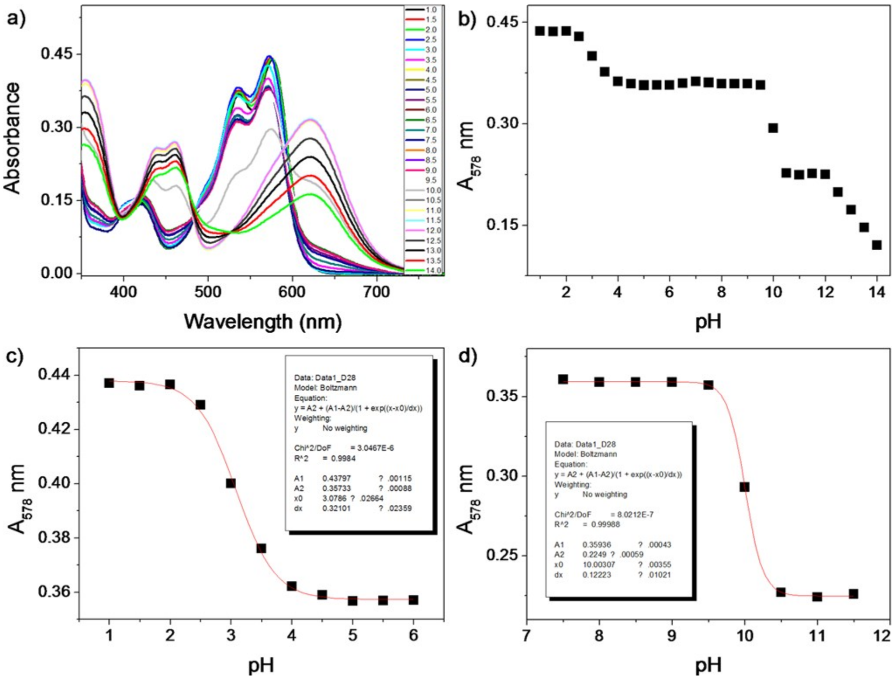

```
Data: Data1_D28
Model: Boltzmann
Equation:
y = A2 + (A1-A2)/(1 + exp((x-x0)/dx))
Weighting:
y           No weighting

Chi^2/DoF        = 3.0467E-6
R^2       =  0.9984

A1        0.43797          ?  .00115
A2        0.35733          ?  .00088
x0        3.0786  ?  .02664
dx        0.32101          ?  .02359
```

```
Data: Data1_D28
Model: Boltzmann
Equation:
y = A2 + (A1-A2)/(1 + exp((x-x0)/dx))
Weighting:
y           No weighting

Chi^2/DoF        = 8.0212E-7
R^2       =  0.99988

A1        0.35936          ?  .00043
A2        0.2249  ?  .00059
x0        10.00307         ?  .00355
dx        0.12223          ?  .01021
```

Fig. S1 Absorption spectra of **1**(10 μM) in different pH solution. a) Absorption spectra of **1** under different pH conditions in water. b) Absorbances of **1** at 578 nm under different pH conditions. c) The pKa (3.01) of the interconversions between cationic and neutral forms derived from the absorbance at 578 nm. d) The pKa (10.0) of the interconversions between neutral and anionic forms derived from the absorbance at 578 nm.

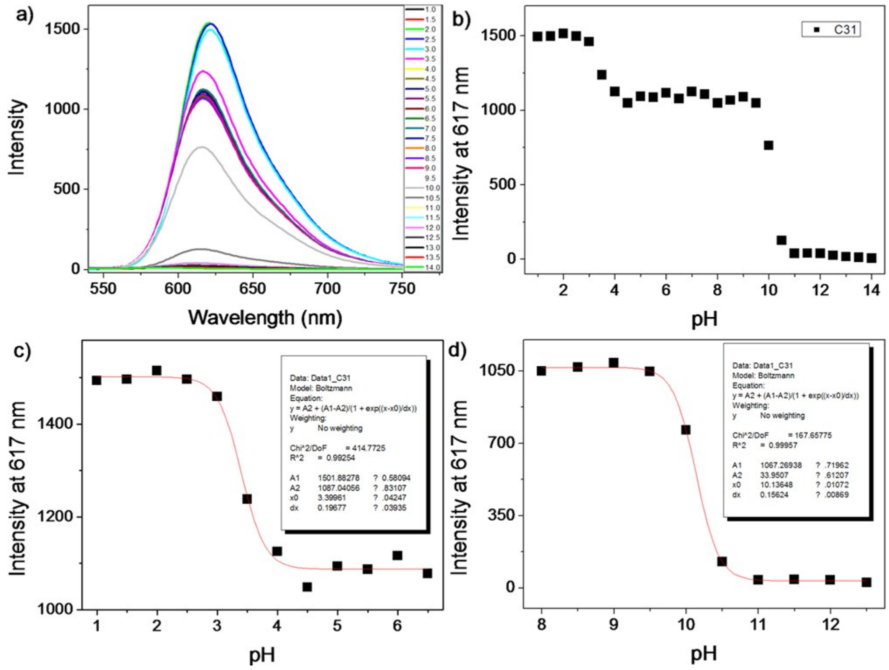

```
Data: Data1_C31
Model: Boltzmann
Equation:
y = A2 + (A1-A2)/(1 + exp((x-x0)/dx))
Weighting:
y           No weighting

Chi^2/DoF        = 414.7725
R^2       =  0.99254

A1        1501.88278       ?  0.58094
A2        1087.04056       ?  .83107
x0        3.39961          ?  .04247
dx        0.19677          ?  .03935
```

```
Data: Data1_C31
Model: Boltzmann
Equation:
y = A2 + (A1-A2)/(1 + exp((x-x0)/dx))
Weighting:
y           No weighting

Chi^2/DoF        = 167.65775
R^2       =  0.99957

A1        1067.26938       ?  .71962
A2        33.9507          ?  .61207
x0        10.13648         ?  .01072
dx        0.15624          ?  .00869
```

Fig. S2 Emission spectra of the dye **1** (5 μM) in different pH solution. a) Emission spectra of **1** under different pH conditions in water. b) Fluorescence intensities of **1** at 617 nm under different pH conditions. c) The pKa (3.4) of the interconversions between cationic and neutral forms derived from the emission intensities at 617 nm. d) The pKa (10.1) of the interconversions between neutral and anionic forms derived from the emission intensities at 617 nm. (λ_{ex} = 540 nm , slit = 5 nm, 10 nm).

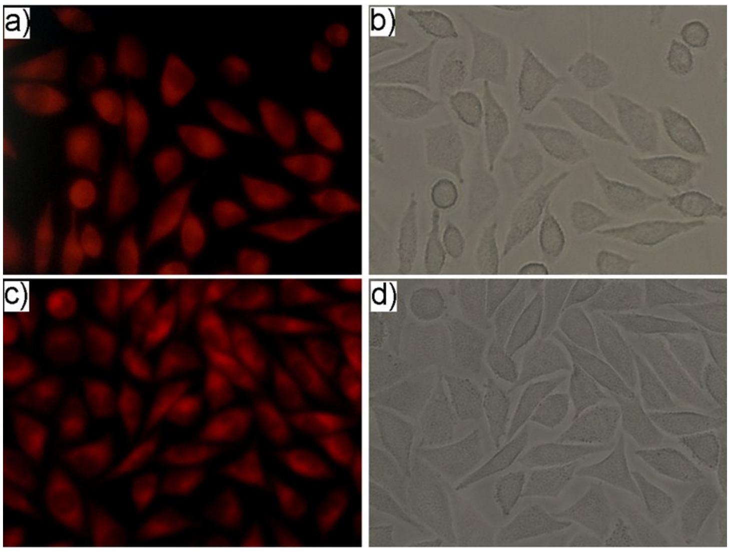

Fig. S3 Images of L929 cells incubated with the dye **1** (15 μM). a) and b) fluorescence and brightfield image after staining for 45 min. c) and d) fluorescence and brightfield image after staining for 24 h.

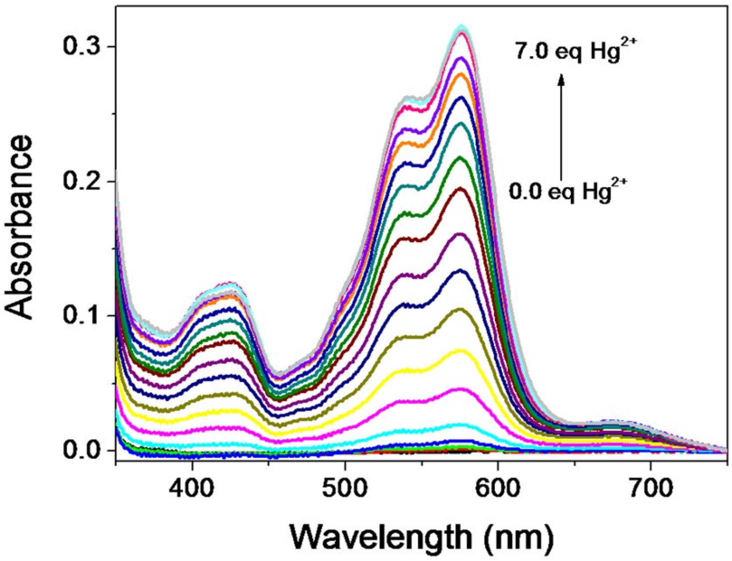

Fig. S4 Absorbance of the hydrazide **5** (5 μM) at varied concentrations of Hg^{2+} in $EtOH/H_2O$ (1:3, v/v).

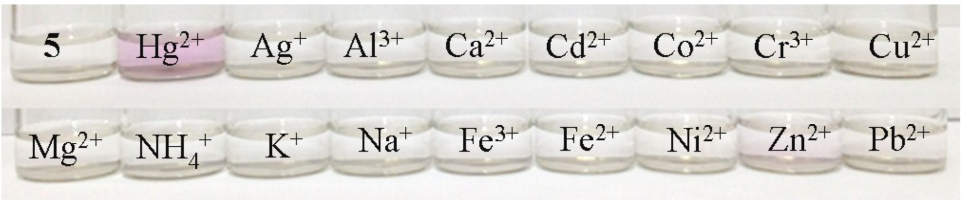

Fig. S5 Color changes of **5** (1×10^{-5} M) in the presence of 5.0 equiv of various ions in ethanol / water (v / v; 1:3).

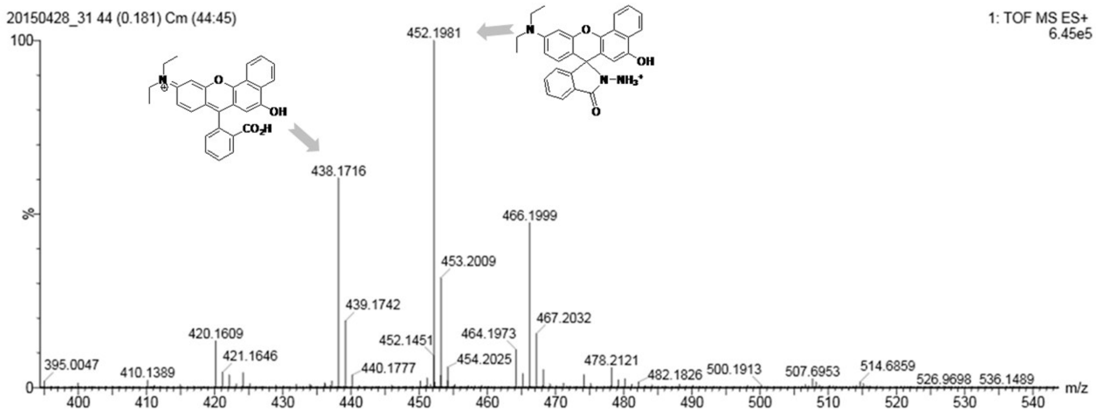

Figure S6. HRMS spectra of the reaction mixture of **5** with Hg^{2+}. The peak (m/z) at 452.1981 corresponds to the chemosensor **5** $[\mathbf{5} + H]^+$ ion (Calcd: 452.1969). The peak (m/z) at 438.1716 corresponds to $[\mathbf{1} + H]^+$ ion (Calcd:438.1705).

Thus, we suggested that the selective optical responsive mechanism was the Hg^{2+}-promoted hydrolysis as shown in the following scheme.

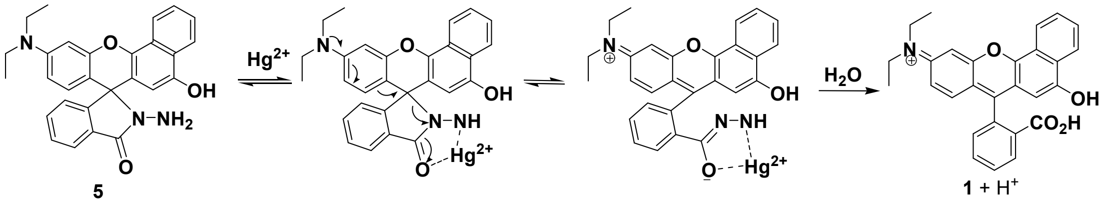

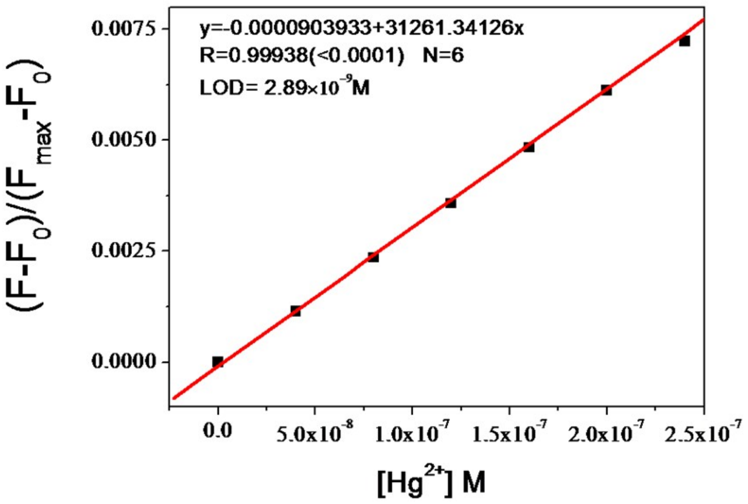

Fig. S7 Emission (at 621 nm) of the hydrazide **5** at different concentrations of Hg^{2+} (0, 0.004, 0.008, 0.012, 0.016, 0.02, 0.024 μM) added, normalized between the minimum emission (0.0 μM Hg^{2+}) and the emission at 0.023 μM Hg^{2+}. The fluorescence intensities were linearly proportional to the amount of Hg^{2+} in this range, and this demonstrated the detection limit is as sensitive as 2.89×10^{-9} M.

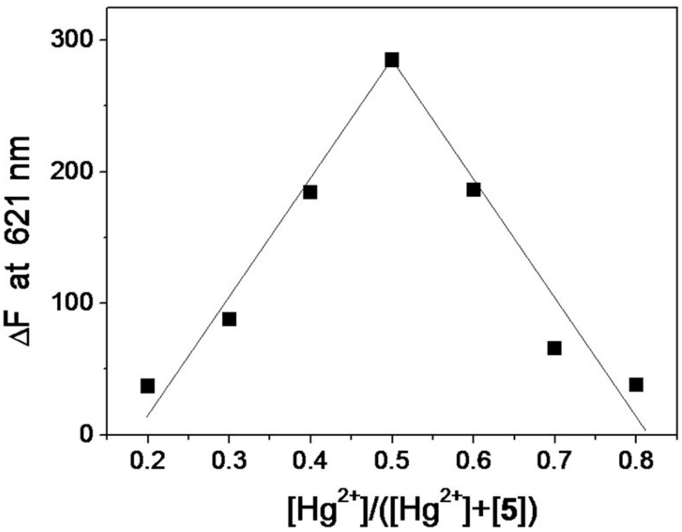

Fig. S8 Job's plot of the interactions between **5** and Hg^{2+} in EtOH/water (1:3, v/v) showing the 1:1 stoichiometry. Total concentration of **5** and Hg^{2+} was kept constant at 10.0 µM. Emission intensity is recorded at 621 nm.

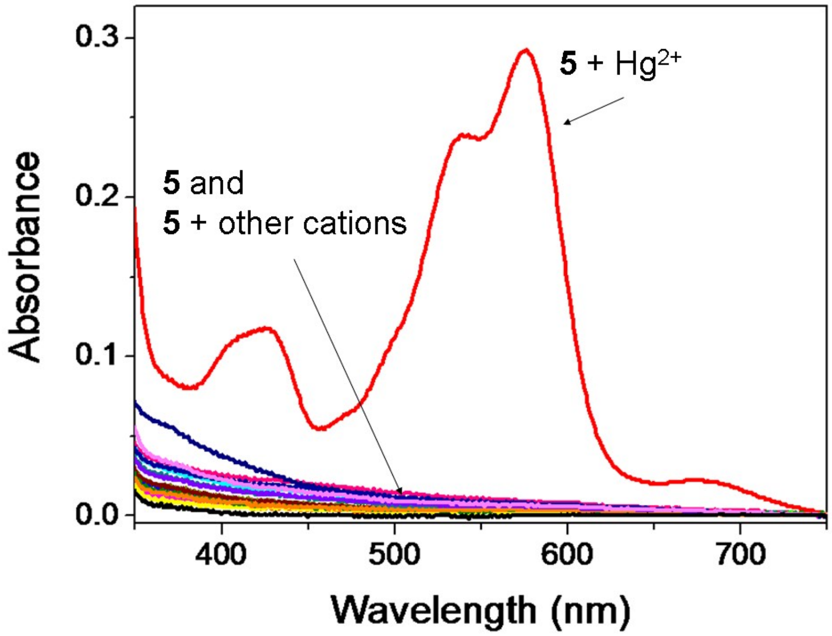

Fig. S9 UV-vis spectra of the hydrazide **5** (10 µM) in the presence of nitrate salts (5.0 equiv) of Na^+, K^+, NH_4^+, Ag^+, Mg^{2+}, Ca^{2+}, Pb^{2+}, Hg^{2+}, Co^{2+}, Cd^{2+}, Zn^{2+}, Ni^{2+}, Cu^{2+}, Cr^{3+}, Fe^{2+}, Fe^{3+}, and Al^{3+} in ethanol/H_2O (v/v, 1:3).

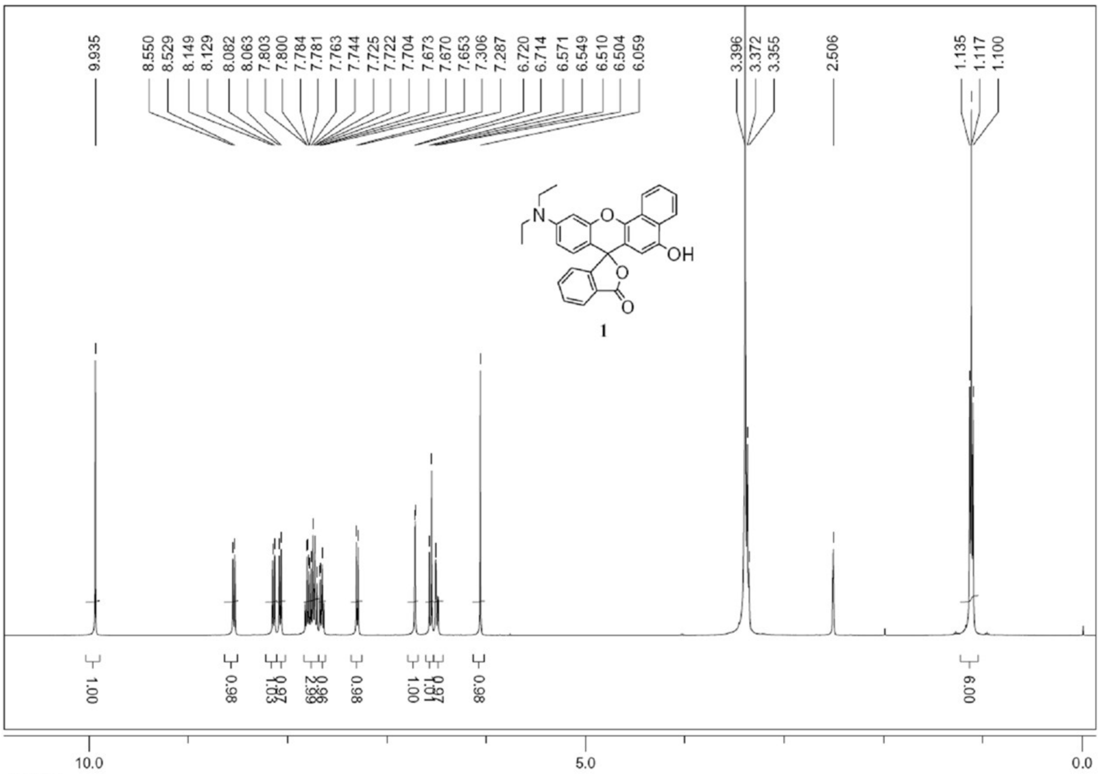

Fig. S10. ^{1}H NMR of **1** (400 MHz, DMSO-d$_6$).

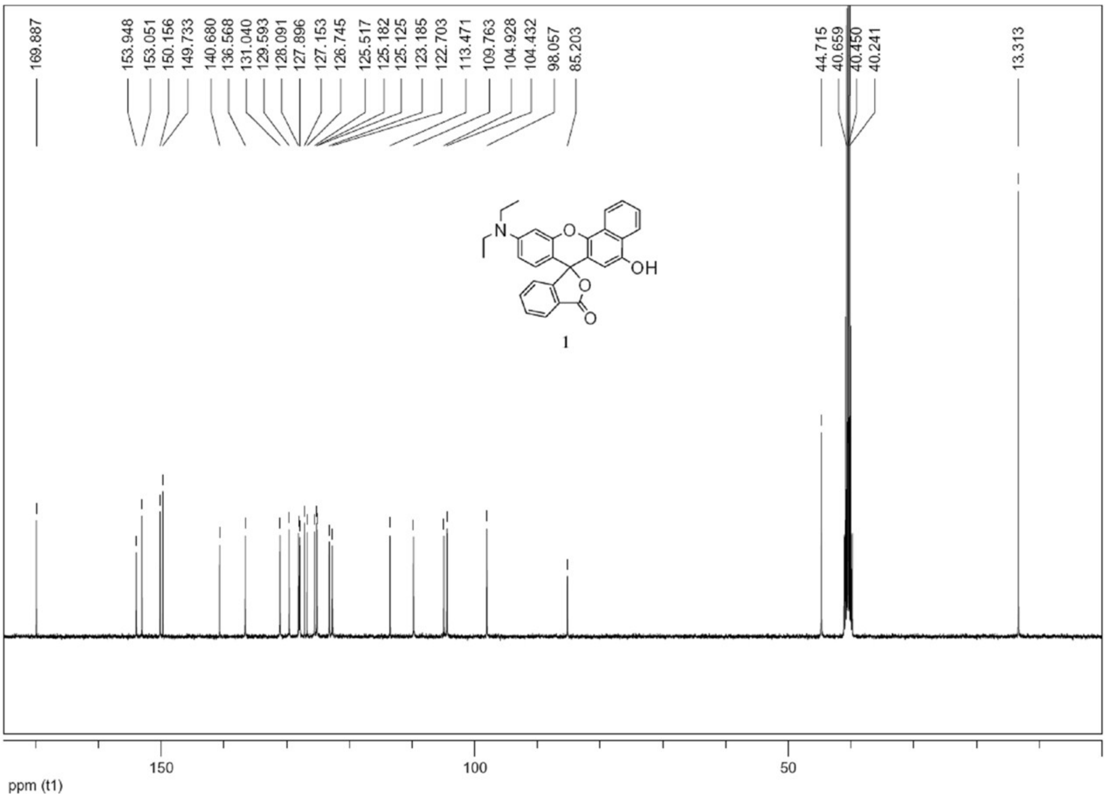

Fig. S11. ^{13}C NMR of **1** (100 MHz, DMSO-d$_6$).

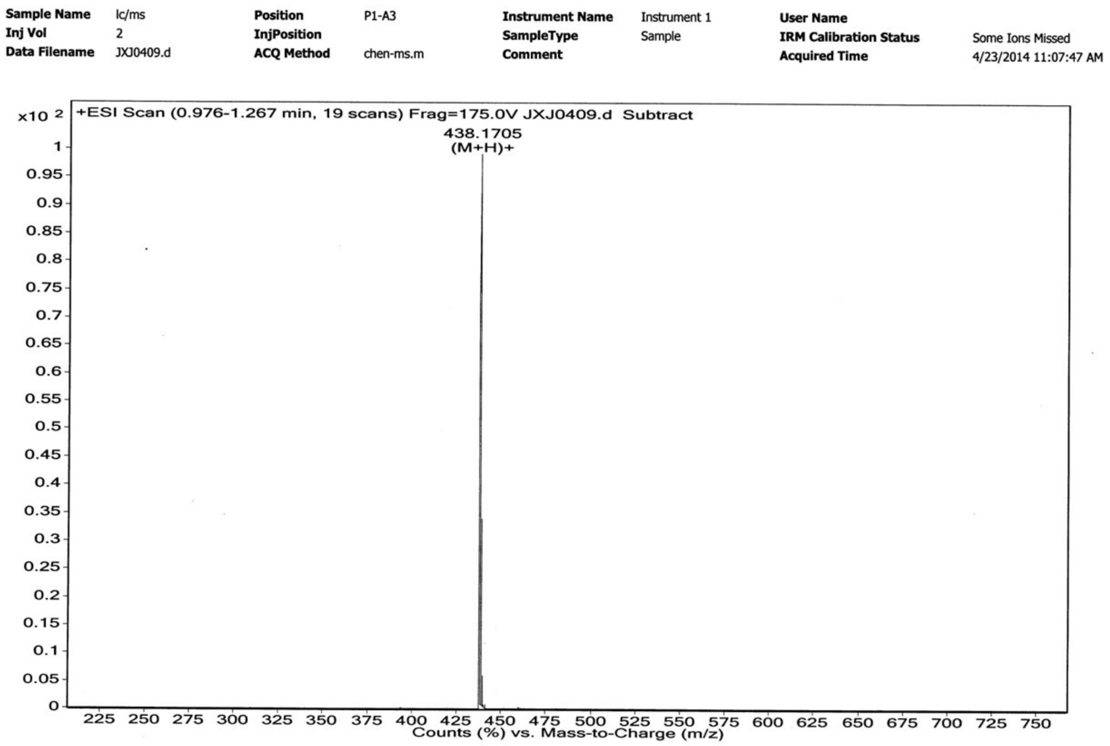

Sample Name	lc/ms	**Position**	P1-A3	**Instrument Name**	Instrument 1	**User Name**	
Inj Vol	2	**InjPosition**		**SampleType**	Sample	**IRM Calibration Status**	Some Ions Missed
Data Filename	JXJ0409.d	**ACQ Method**	chen-ms.m	**Comment**		**Acquired Time**	4/23/2014 11:07:47 AM

Fig. S12. HRMS (LC/MS) spectra of **1**. The peak at m/z = 438.1705 was assigned to the mass of **1**+H$^+$.

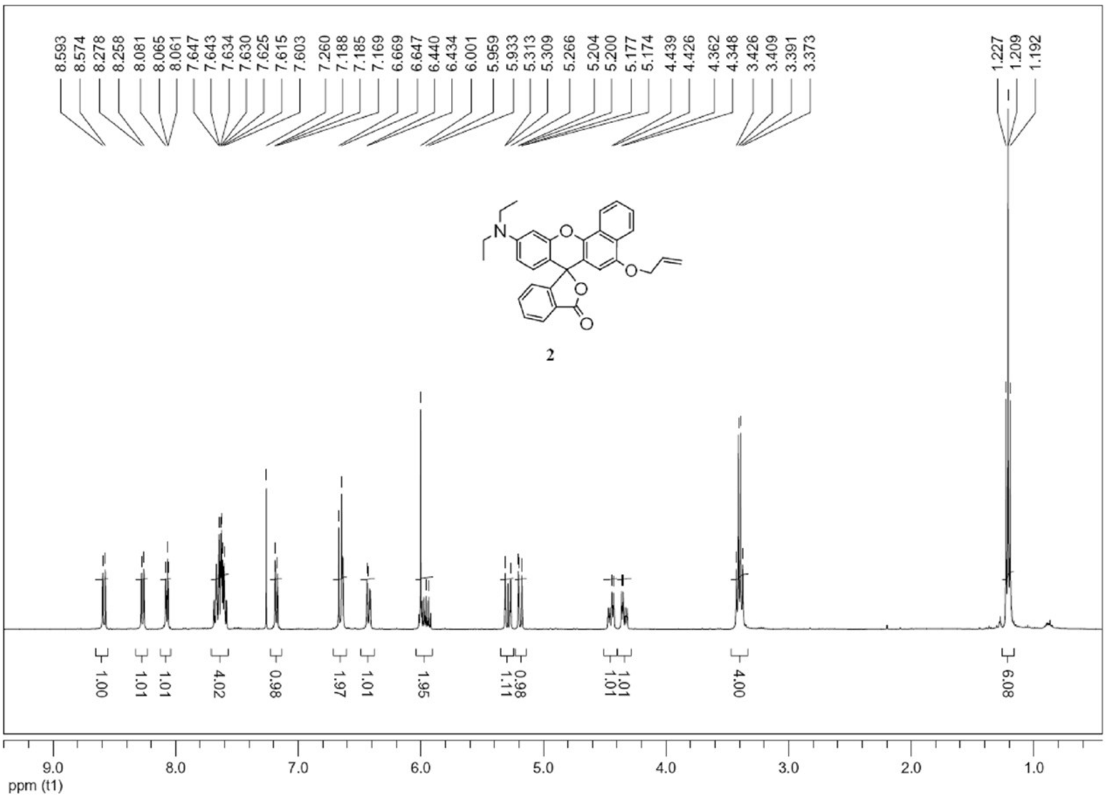

Fig. S13. ^{1}H NMR of **2** (400 MHz, CDCl$_3$).

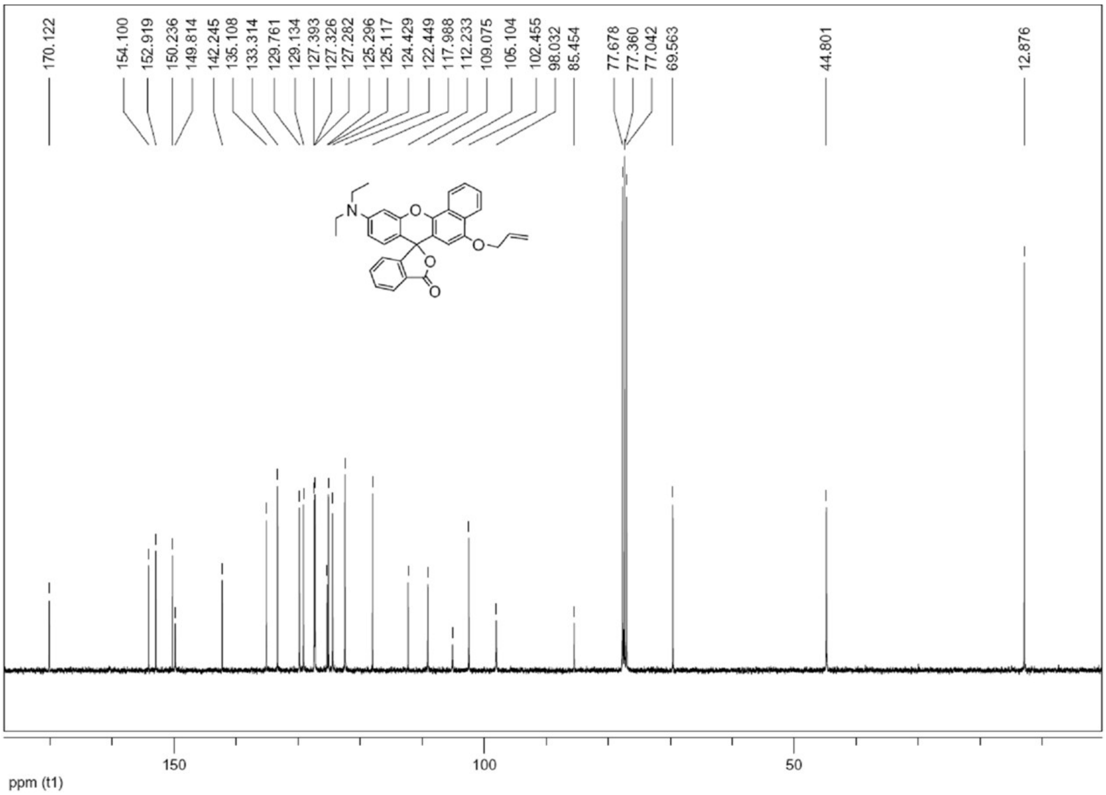

Fig. S14. ^{13}C NMR of **2** (100 MHz) in $CDCl_3$.

Sample Name	lc/ms	**Position**	P1-A7	**Instrument Name**	Instrument 1	**User Name**	
Inj Vol	2	**InjPosition**		**SampleType**	Sample	**IRM Calibration Status**	Some Ions Missed
Data Filename	JXJ0415.d	**ACQ Method**	chen-ms.m	**Comment**		**Acquired Time**	4/28/2014 12:51:33 PM

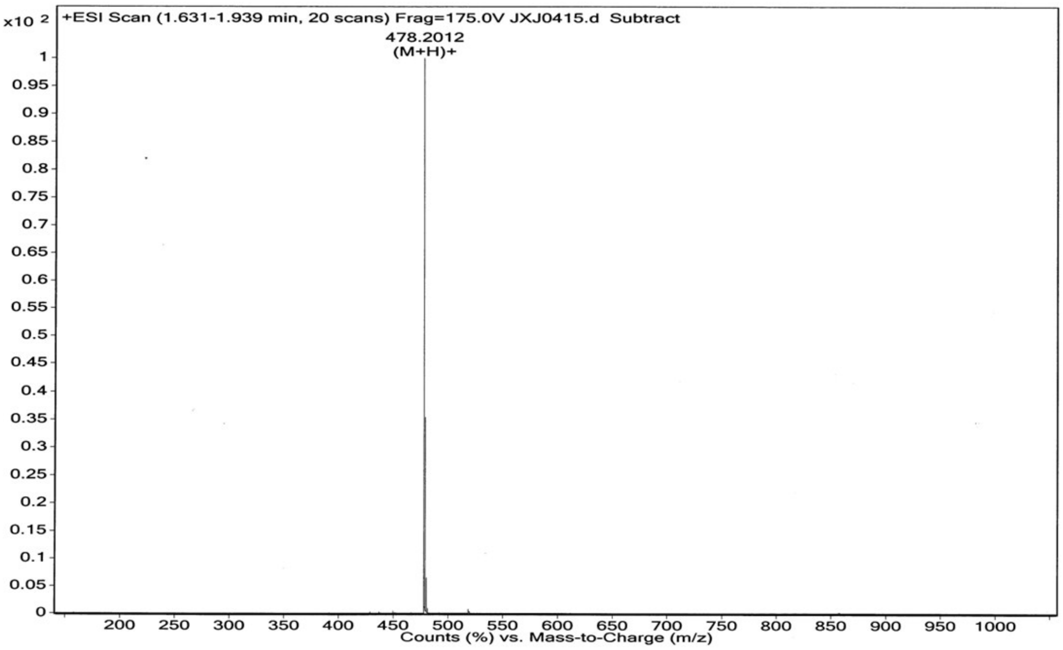

Fig. S15. HRMS (LC/MS) spectra of **2**. The peak at m/z = 478.2012 was assigned to the mass of **2**+H^+.

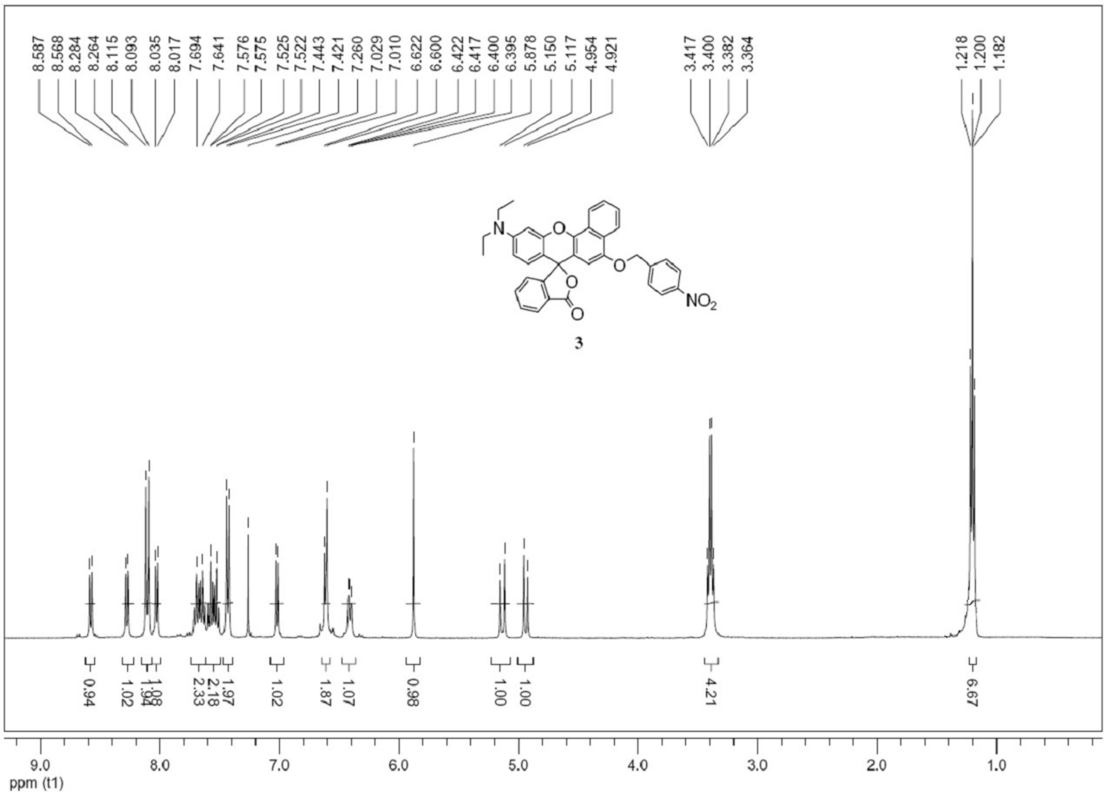

Fig. S16. ^{1}H NMR of **3** (400 MHz, CDCl$_3$).

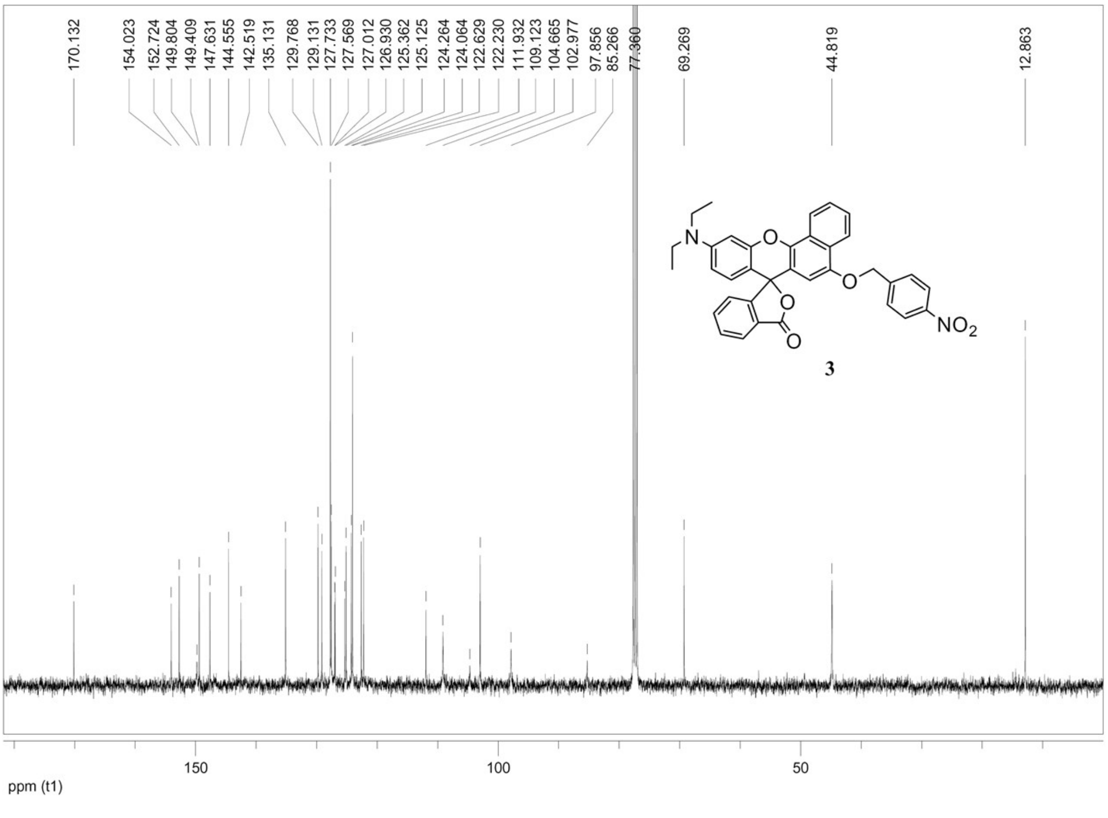

Fig. S17. ^{13}C NMR of **3** (100 MHz) in CDCl$_3$

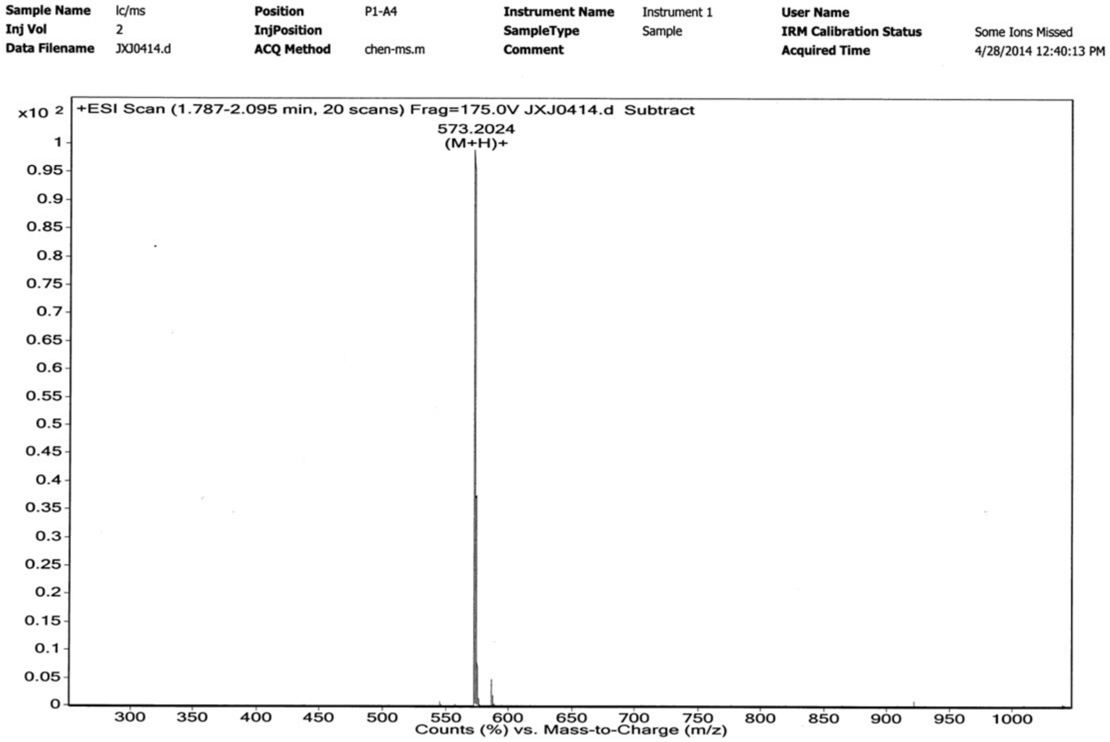

Sample Name	lc/ms	**Position**	P1-A4	**Instrument Name**	Instrument 1	**User Name**	
Inj Vol	2	**InjPosition**		**SampleType**	Sample	**IRM Calibration Status**	Some Ions Missed
Data Filename	JXJ0414.d	**ACQ Method**	chen-ms.m	**Comment**		**Acquired Time**	4/28/2014 12:40:13 PM

Fig. S18. HRMS (LC/MS) spectra of **3**. The peak at m/z = 573.2024 was assigned to the mass of **3**+H$^+$.

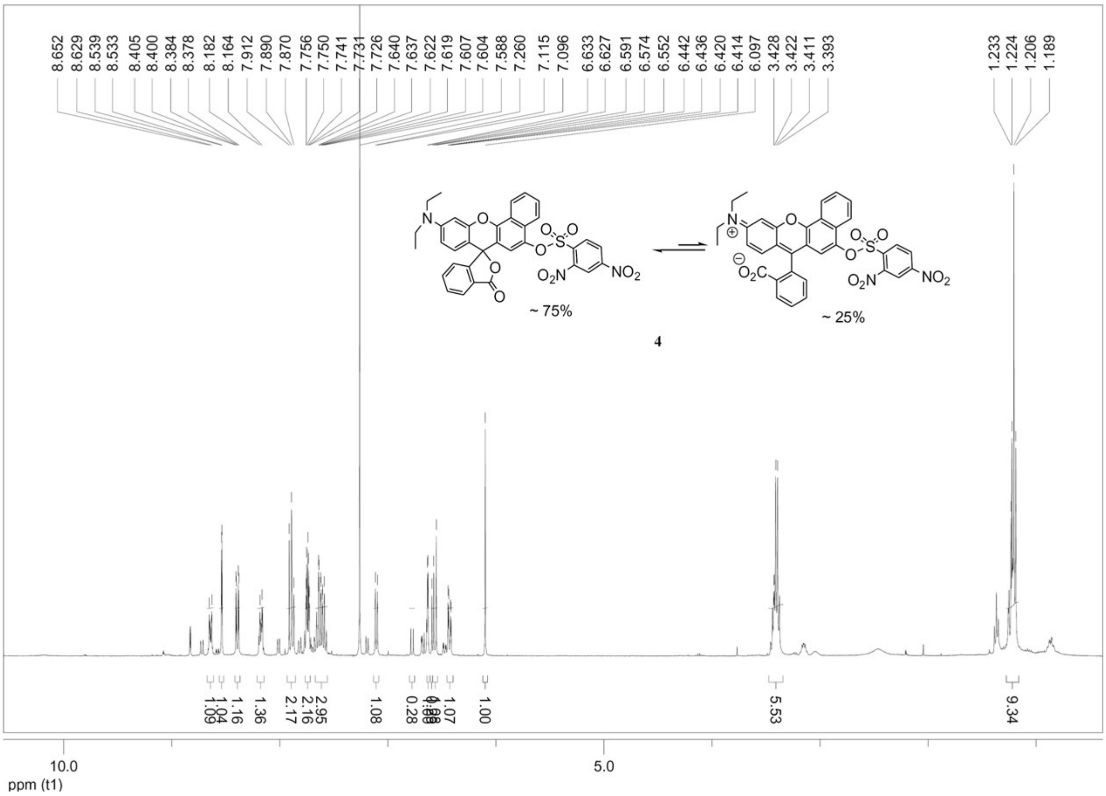

Fig. S19. ^1H NMR of **4** (400 MHz, $CDCl_3$).

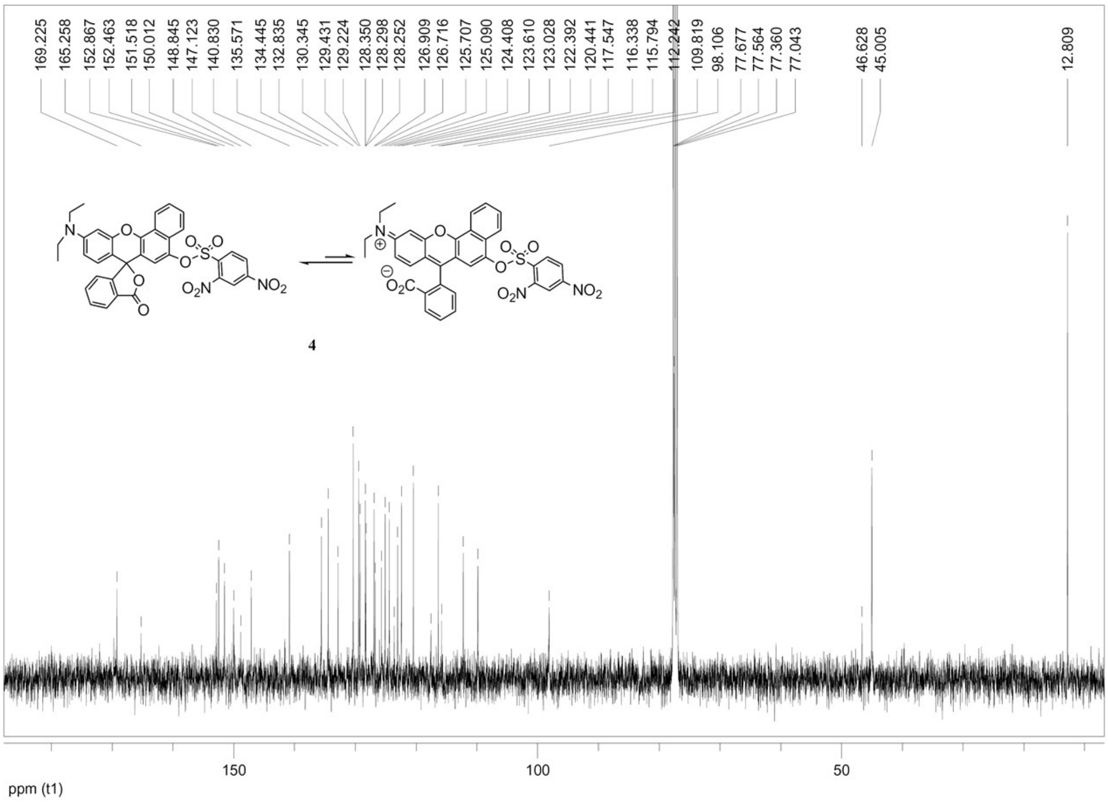

Fig. S20 ^{13}C NMR of **4** (100 MHz) in $CDCl_3$

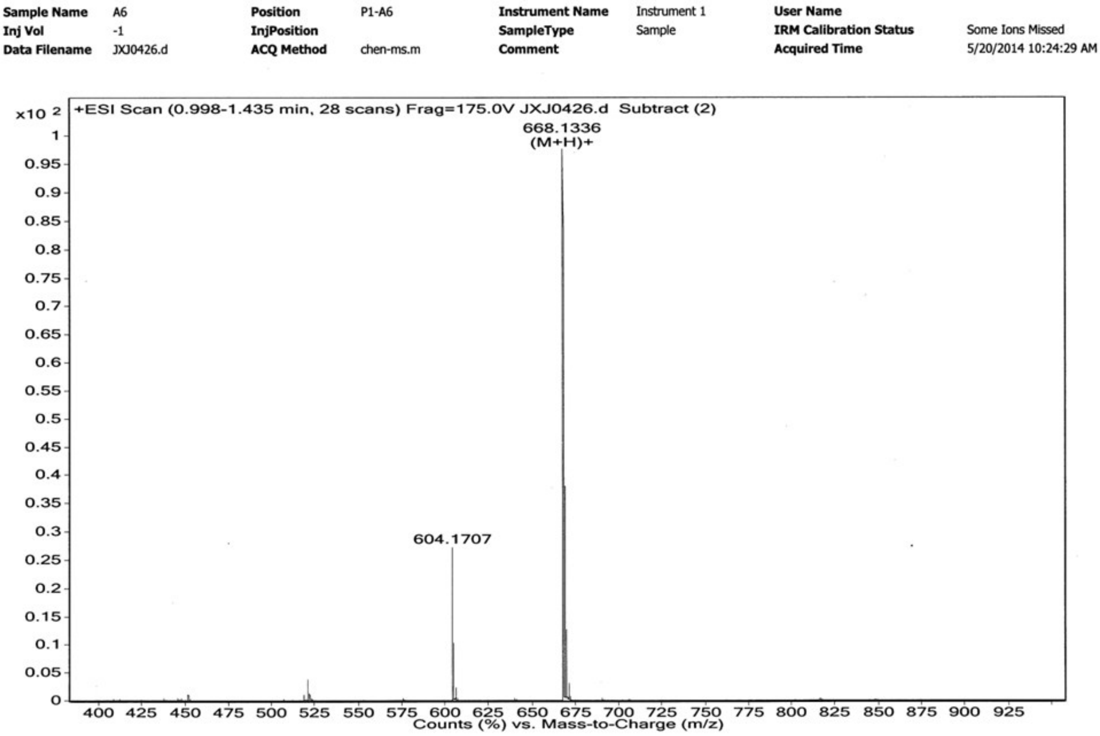
Sample Name A6 **Position** P1-A6 **Instrument Name** Instrument 1 **User Name**
Inj Vol -1 **InjPosition** **SampleType** Sample **IRM Calibration Status** Some Ions Missed
Data Filename JXJ0426.d **ACQ Method** chen-ms.m **Comment** **Acquired Time** 5/20/2014 10:24:29 AM

Fig. S21 HRMS (LC/MS) spectra of **4**. The peak (m/z) at 668.1336 and the peak (m/z) at 604.1707 corresponded $(M + H)^+$ and $(M + H - SO_2)^+$, respectively.

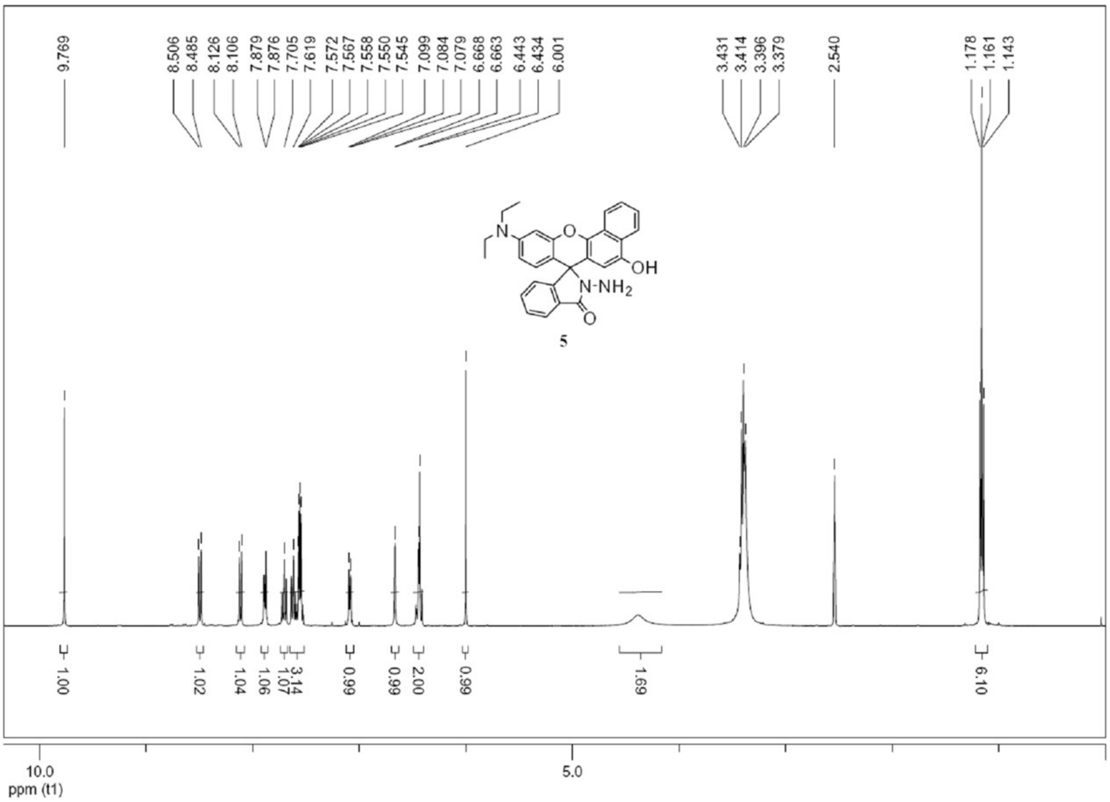

Fig. S22 ^{1}H NMR of **5** (400 MHz, DMSO-d$_6$).

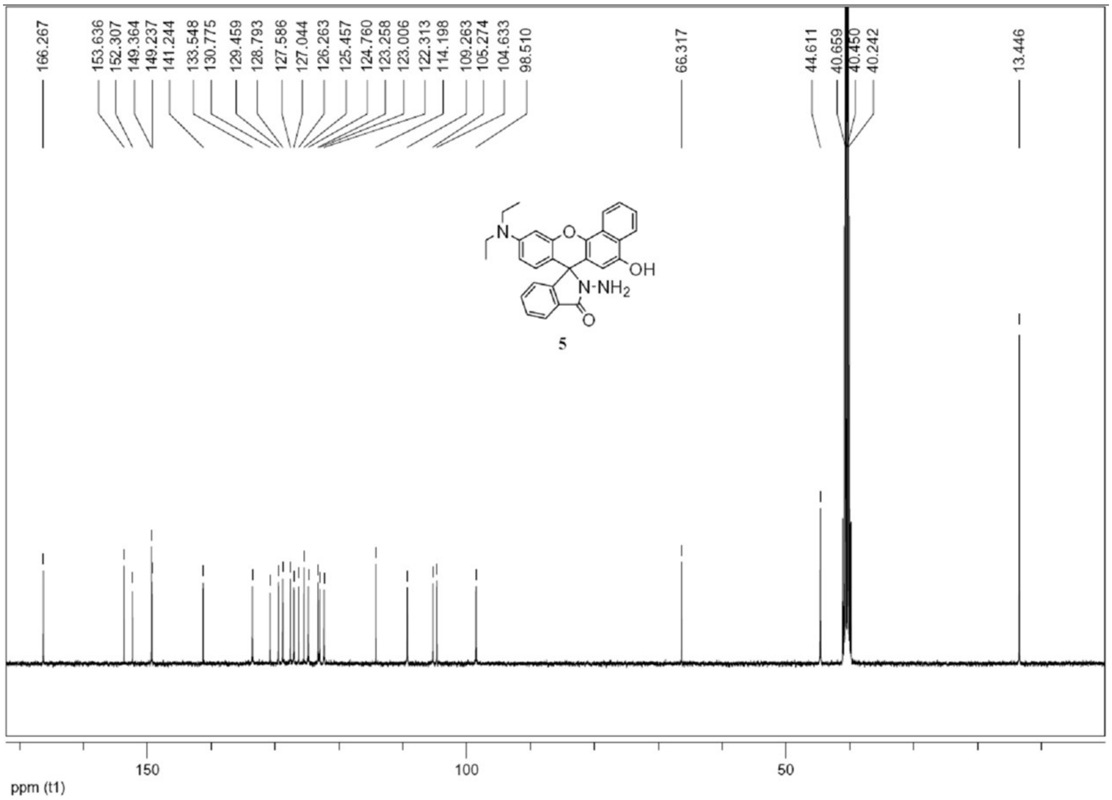

Fig. S23 ^{13}C NMR of **5** (100 MHz) in DMSO-d$_6$

Sample Name	A8	**Position**	P1-A8	**Instrument Name**	Instrument 1	**User Name**	
Inj Vol	-1	**InjPosition**		**SampleType**	Sample	**IRM Calibration Status**	Some Ions Missed
Data Filename	JXJ0511.d	**ACQ Method**	chen-ms.m	**Comment**		**Acquired Time**	5/20/2014 10:32:02 AM

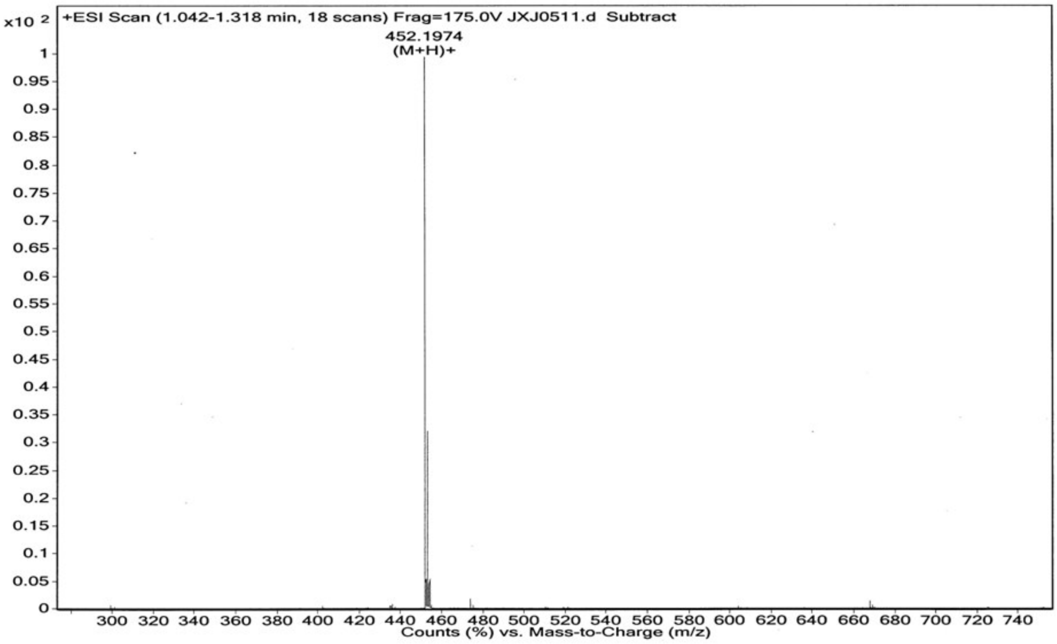

Fig. S24 HRMS (LC/MS) spectra of **5.** The peak (m/z) at 452.1974 corresponded $(M + H)^+$.